Bulletin of the Geological Survey of Japan, vol. 39(1), p.39-61, 1988 551.217/.352 (528.1)

Sedimentation of the Sumisu Rift, Izu-Ogasawara Arc

Akira NISHIMURA* and Fumitoshi MURAKAMI*

NISHIMURA, A. and MURAKAMI, F. (1988) Sedimentation of the Sumisu Rift, Izu-Ogasawara Arc. *Bull. Geol. Surv. Japan*, vol. 39(1), p.39-61.

Abstract : Sediment cores obtained from the Sumisu Rift (composed of two separated basins, the North and the South Basins) of the Izu-Ogasawara (Bonin) Arc are described and analyzed with the objective of determining their origins and sedimentation processes with the 3.5-kHz echogram analysis. The sediments in the core sequences are roughly divided into two lithologic units, hemipelagic mud and turbidites composed mainly of volcaniclastics from arc volcanoes.

In the South Basin, the thick transparent layer on SBP records covers the whole basin floor. The surface sediments of this basin are composed of lithologic units mentioned above and correspond to the transparent layer on SBP records, and the lithology expressed by the sharp multiple reflectors below the transparent layer is possibly correlated to the hemipelagic mud with high content of calcium carbonate accompanying some volcanogenic sediment layers.

In the North Basin, echogram suggests that gravity flows, such as sliding, debris flow, and turbidity flow, played important roles during sedimentation. But sediment core lithology is almost the same as that of the South Bashin, except for the larger content of coarser volcanogenic turbidites.

1. Introduction

Sedimentation models in marginal basins (back arc basins) are constructed mainly on DSDP data (KARIG and MOORE, 1975 ; CAREY and SIGURDSSON, 1984). It is pointed out that the combination of arc volcanic activity and tectonics of the basin being formed decide the nature of sediments of marginal basins and that the depositional stages are divided by the contribution of volcanogenic and biogenic components to the sediments.

The Sumisu Rift is located in the middle part of the Izu-Ogasawara Arc. It is included in "the back-arc depressions" forming a discontinuous line along the volcanic chain of the arc. TAMAKI *et al.* (1981) pointed out that they constitute active spreading systems showing the commencement of back arc rifting. Recently, closely spaced seismic and sampling survey was conducted by the Geological Survey of Japan (Geological Survey of Japan, 1985 ; NAKAO and YUASA, 1986, 1987). This paper reports the results of the sediment sample analysis and the estimation of the sedimentary processes in the Sumisu Rift. It is based on the data and samples obtained by the Geological Survey of Japan.

*Marine Geology Department

2. Topography of the Sumisu Rift

The Sumisu Rift is located immediately west of the Shichito volcanic chain between the Sumisu Jima and the Tori Shima Islands (Fig.1). The rift is composed of two basins, the North and the South Basins[1)], separated

1) The North and the South Basins are called the Kita-Sumisu Basin and the Minami-Sumisu Basin, respectively, in the bathymetric chert "Sumisu Sima (No.6527)" published by the Maritime Safety Agency.

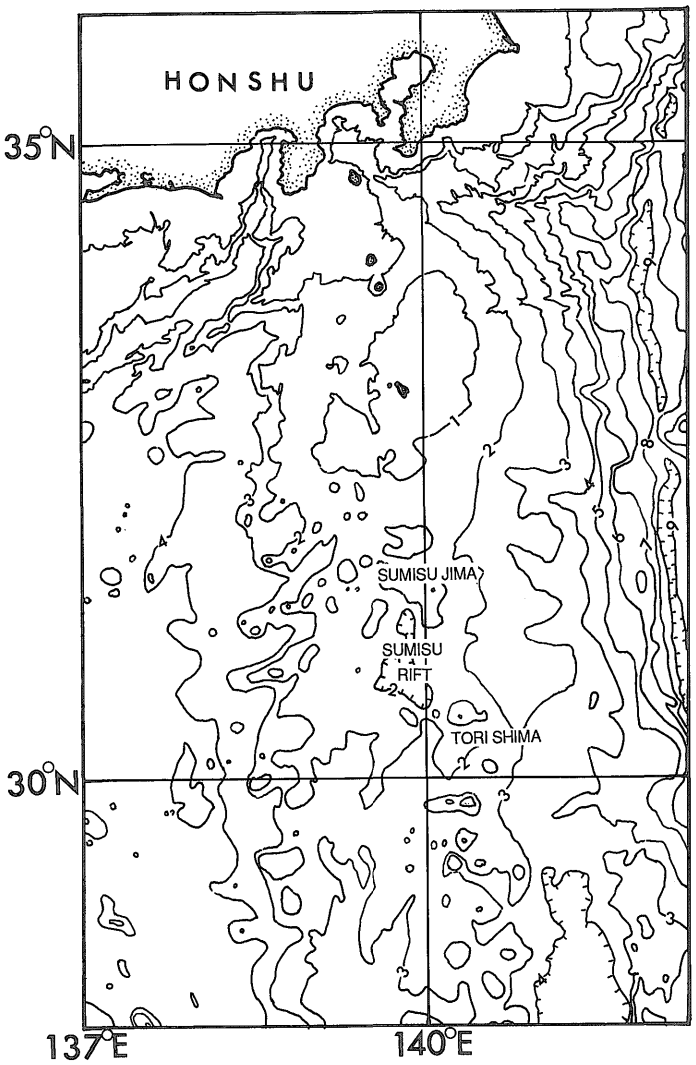

Fig. 1 Index map of the Sumisu Rift. Depth in km.

by the association of intra-rift volcanoes (BROWN and TAYLOR, 1988) (Fig.2).

The North Basin has the dimension of 15× 30 km and is elongated in N-S direction. The basin has a very steep fault scarp on the eastern side and a gentle slope on the western side. Basin floor shows undulation and inclined flat in several places. Restricted flat basin floor is also observed in the western part with a N-S trend. Average depth of the North Basin is about 2100m deep.

The dimension of the South Basin is 35× 45 km. The basin has also a steep fault scarp on the eastern side and a relatively gentle slope on the western side. The southern margin of the basin where the basin structurally continued to the Torishima Depression, is formed by the line of mountains east of the Tori Shima Island. The basin3. floor is wide and faulted and is about 2250m deep. The basin is filled with thick sediment layers. The thickness exceeds 1.2sec. two-

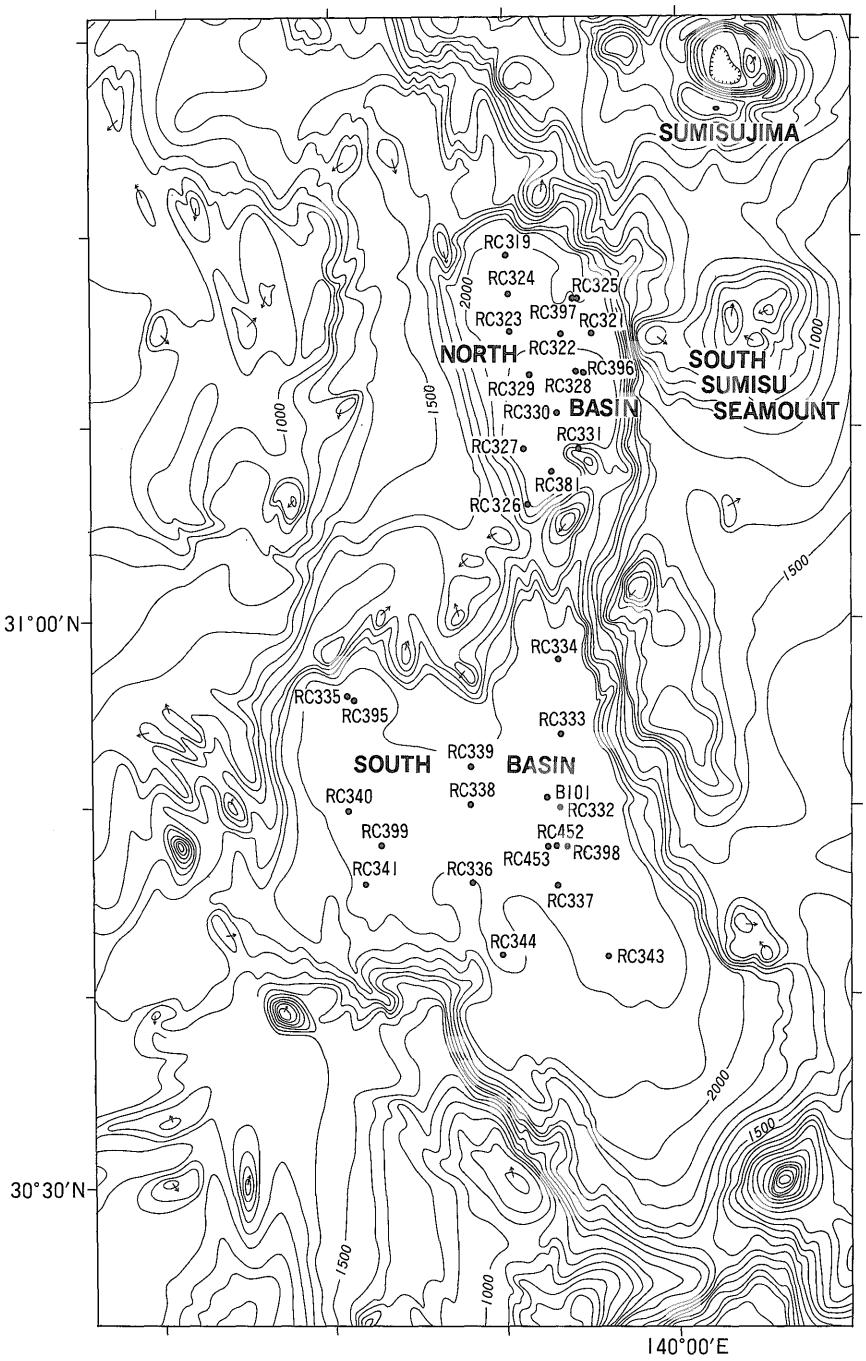

Fig. 2 Topography and sampling locations of the Sumisu Rift. Bathymetric map is based on Geological Survey of Japan (1985). Depth in meters.

way travel time on air-gun profiles (MURAKAMI, 1988) at the west central part of the South Basin where the rifting axis has a N-S trend (MURAKAMI, 1988 ; BROWN and TAYLOR, 1988). Many N-S trending faults which indicate rifting sometimes cut the uppermost sediment layer.

3. Material and Methods

The sediment samples were collected mainly during the GH84-2 Cruise and also during the GH85-1, GH85-3 and GH86-1 Cruises. A short gravity corer with 2 meter core barrel (a rock corer) was used. Fine volcaniclastic sediments at less than a meter below the sea floor hamper the penetration of the corer. Thus most core sequences are less than one meter. These sediments will be described later. The sampling stations are shown in Figure 2 and Table 1.

The sediment cores were visually described and compositions were determined mainly through smear slide observation. Compositions of the coarser part of the sediments were determined through the binocular microscopic observation of sieved residue with 63 μ m openings. Sedimentary structures were observed in the X-radiograph using 1 cm thick vertical slices. Grain size distributions were analyzed by sieving and gravimetric (hydrometer) method on some samples. Calcium carbonate were measured using the weight loss in hydrochloride solution on the base of sediment dry weight.

Bathymetric and seismic (air gun and sub-bottom profiler) data were used for the study on the interpretation of the sedimentation processes. Seismic survey was carried out along E-W and N-S trending survey lines with intervals of 2 to 4 nautical miles, mainly during the GH 84-2 Cruise (MURAKAMI, 1988) (Fig.3). High-frequency (3.5-kHz SBP) echograms provide useful data for the near bottom sedimentation processes on the deep-sea floor in combination with other data(cores, bottom photographs, nephrometer, etc.) (DAMUTH, 1980). Sediment slide complex had been successfully mapped using echograms (JACOBI, 1976). Echocharacter mapping of the Sumisu Rift was carried out on the same echogram data of this study in combination with SeaMARC II image data (BROWN and TAYLOR, 1988). Then in this study, attempts

Table 1 Sampling location data in the Sumisu Rift.

Sample No.	Latitude (N)	Longitude (E)	Water depth (m)
North basin			
R C 319	31°19.08′	139°50.18′	2052
R C 324	31°17.03′	139°50.23′	2075
R C 323	31°15.13′	139°50.33′	2100
R C 325	31°16.84′	139°54.21′	2048
R C 397	31°16.87′	139°53.99′	2045
R C 322	31°14.97′	139°53.36′	2105
R C 321	31°15.09′	139°55.13′	2087
R C 329	31°12.87′	139°51.50′	2127
R C 328	31°13.01′	139°54.28′	2125
R C 396	31°12.92′	139°54.63′	2123
R C 330	31°10.81′	139°53.11′	2136
R C 327	31°08.94′	139°51.21′	2137
R C 331	31°08.90′	139°54.43′	2136
R C 381	31°07.67′	139°52.76′	2135
R C 326	31°05.98′	139°51.32′	2119
South basin			
R C 334	30°57.94′	139°53.13′	2279
R C 333	30°54.00′	139°53.37′	2278
R C 335	30°55.87′	139°40.84′	2221
R C 395	30°55.73′	139°41.23′	2220
R C 339	30°52.33′	139°48.20′	2212
R C 338	30°50.05′	139°48.06′	2231
B 101	30°50.46′	139°52.29′	2275
R C 332	30°49.98′	139°53.14′	2286
R C 398	30°47.86′	139°53.56′	2293
R C 452	30°47.97′	139°53.13′	2270
R C 453	30°47.97′	139°52.44′	2260
R C 337	30°45.89′	139°52.98′	2262
R C 343	30°42.09′	139°55.87′	2287
R C 344	30°42.27′	139°49.96′	2220
R C 336	30°45.99′	139°47.99′	2187
R C 340	30°49.82′	139°40.87′	2228
R C 399	30°47.94′	139°42.72′	2235
R C 341	30°46.01′	139°41.72′	2224

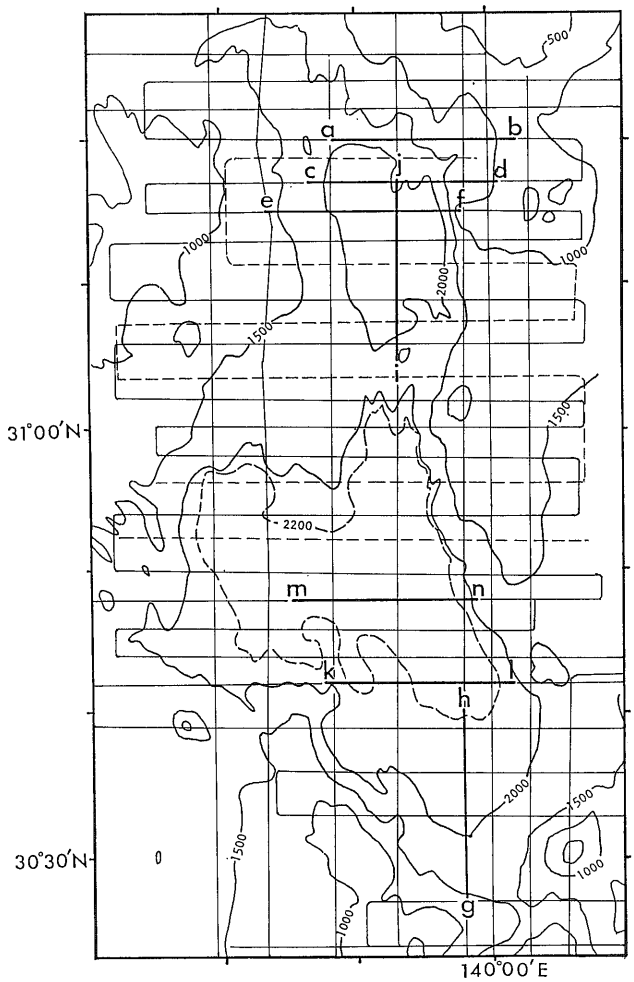

Fig. 3 Seismic survey lines used for 3.5 kHz echogram analysis. Straight lines are survey lines during the GH84-2 Cruise. Broken lines are survey lines during the GH80-4 Cruise which have 3.5 kHz SBP with poor resolution. Thick lines show survey lines of examples in Fig. 4. Depth in meters.

were made to interpret sedimentation processes from the echogram characteristics particularly in consideration of the succession of the echogram types and the relationship between the echogram types and topographic nature.

4.. Results

4.1 Echogram types

Nine echogram types can be distinguished by the characteristics of the bottom and sub-bottom reflectors in and around the basins mostly based on the classification of JACOBI (1976) and DAMUTH (1980). These types are thought to be related to the sedimentary processes, and association and arrangement of echogram types are useful to interpret the sedimentary processes. Arrangement of slide scar, hummocky terrane, blocky terrane, and debris flow, which is observed in a downslope sequence related to the sediment slide deposition (JACOBI, 1976) possibly corresponds to that of Types A, C, D, and E in

this area described below. Descriptions of the types with interpretations (JACOBI, 1976, DAMUTH, 1980) and examples of profiles (Fig.3) are shown in Table 2 and Figures 4(1)-(7). Types are :

Type A; irregular overlapping hyperbolae with varying vertex elevations above the seafloor on steep slopes (Fig. 4-(1)). Hyperbolae echograms similar to this type occur in various places around the basins, but very crowded hyperbolae echogram, which can be interpreted as a structure related to sliding sedimentation, is picked up as Type A.

Type B; irregular overlapping hyperbolae with varying vertex elevations above the seafloor on basin floors (Figs.4(1) and 4(2)). This type has the same echogram feature as that of type A, but occurrs on the basin floors. Seismic profiles of the area with this echogram type shows chaotic feature suggesting sliding sedimentation of large blocks (MURAKAMI, 1988).

Type C; regular overlapping hyperbolae with vertices approximately tangent to seafloor (Fig.4(3) and 4(4)). This type occurrs on gentle slopes and the roughness of the bottom reflector suggests that this type shows debris flow deposits with small blocks.

Type D; very prolonged, fuzzy bottom reflector with no subbottom reflectors (Figs.4(2), 4(3) and 4(4)). This type often occurrs on the down-slope side of type C and possibly shows debris flow deposits.

Type E; transparent wedge with prolonged subbottom reflectors (Figs.4(4), 4(5) and 4(6)). The transparency may indicate the highly deformed/fluidized nature of the debris flow (JACOBI, 1976). This type occurs on the down-slope side of type D and forms a small wedge along the fault.

Type F; semi-prolonged bottom reflector (Fig.4(6)). This type distributes in N-S trending narrow depressions along the faults surrounded by echogram types of sharp reflector with distinct transparent part (Type H). This type is distinct at the southern margin of the South Basin but it disappears northward. The distribution of this type suggests that this type shows turbidite fill restricted in channels.

Type G; semi-prolonged bottom reflector with discontinuous, parallel subbottom reflectors (Fig. 4(5)). Cores taken from the area with this echogram type of the East Brazilian Margin yield silt/sand layers of distal turbidites (JACOBI, 1976). This type occupies the deepest part of the basin floor of the North Basin and the basin floor is almost flat, which suggest that this type shows turbidite fill in basin floor.

Type H; sharp, continuous bottom reflector with distinct transparent part with the subbottom reflectors (Figs. 4(6) and 4(7)). Transparent part is quite uniform in the South Basin. The thickness of the transparent part tends to be thick in depressions and thin on topographic elevations, which suggests that this type is formed by pelagic sedimentation slightly modified by bottom currents.

Type I; sharp, continuous, multiple reflectors (Figs. 4(6) and 4(7)). The pattern of the multiple layers is uniform. This type is correlated to the lower part of Type H echogram and restrictedly crops out along the faults. The layered pattern of this type shows parallel to undulated topography, which suggests that this type is related to pelagic sedimentation.

4.2 Lithologic units

Brief descriptions of the sediment cores of this area have already been published (Geological Survey of Japan, 1985; NAKAO and YUASA, 1986, 1987). On the basis of visual

Table 2 Echogram types identified in and around the Sumisu Rift.

TYPE	ECHO CHARACTERS	TOPOGRAPHY(inclination)	INTERPRETATIONS	DISTRIBUTION	REFERENCES
(A)	Irregular overlapping hyperbolae with varying vertex elevations above sea floor on steep slopes	steep slope (-7°)	sliding scars sliding blocks	north-east of North Basin (NB)	Slide scars, Hummocky terrane (JACOBI, 1976) IIIC (DAMUTH, 1980)
(B)	Irregular overlapping hyperbolae with varying vertex elevations above sea floor on basin floors	basin floor foot of slope (almost flat)	sliding blocks	north-eastern part of NB	IIIC (DAMUTH, 1980)
(C)	Regular overlapping hyperbolae with vertices approximately tangent to sea floor	gentle slope (7-3°)	slide scars debris (blocky) flow deposits	western slope of NB south-eastern slope of South Basin (SB)	Blocky terrane (JACOBI, 1976) IIID (DAMUTH, 1980)
(D)	Very prolonged, fuzzy bottom reflector with no subbottom reflector	very gentle slope (3-1°)	debris flow deposits	eastern & western parts of NB and south-eastern slope of SB	Debris flow (JACOBI, 1976) IIB (DAMUTH, 1980)
(E)	Transparent wedge with prolonged subbottom reflector	foot of slope basin floor (1°-)	debris (mud) flow deposits	central part of NB and southern margin of SB	Debris flow (JACOBI, 1976)
(F)	Semi-prolonged bottom reflector	basin floor (almost flat)	turbidite filling	eastern part of SB	Turbidity flow pathway (JACOBI, 1976) (IIA)(DAMUTH, 1980)
(G)	Semi-prolonged bottom reflector with discontinuous, parallel subbottom reflectors	basin floor (almost flat)	turbidite filling	north-western & south-western parts of NB	IIA (DAMUTH, 1980)
(H)	Sharp, continuous bottom reflector with distinct transparent part with subbottom reflectors	basin floor (almost flat)	hemipelagic drape (with pyroclastic layers)	whole area of SB	Normal hemipelagic sedimentation (JACOBI, 1976) IB (DAMUTH, 1980)
(I)	Sharp, continuous, multiple reflectors	basin floor (almost flat)	hemipelagic drape with pyroclastic layers	south-eastern part of SB	

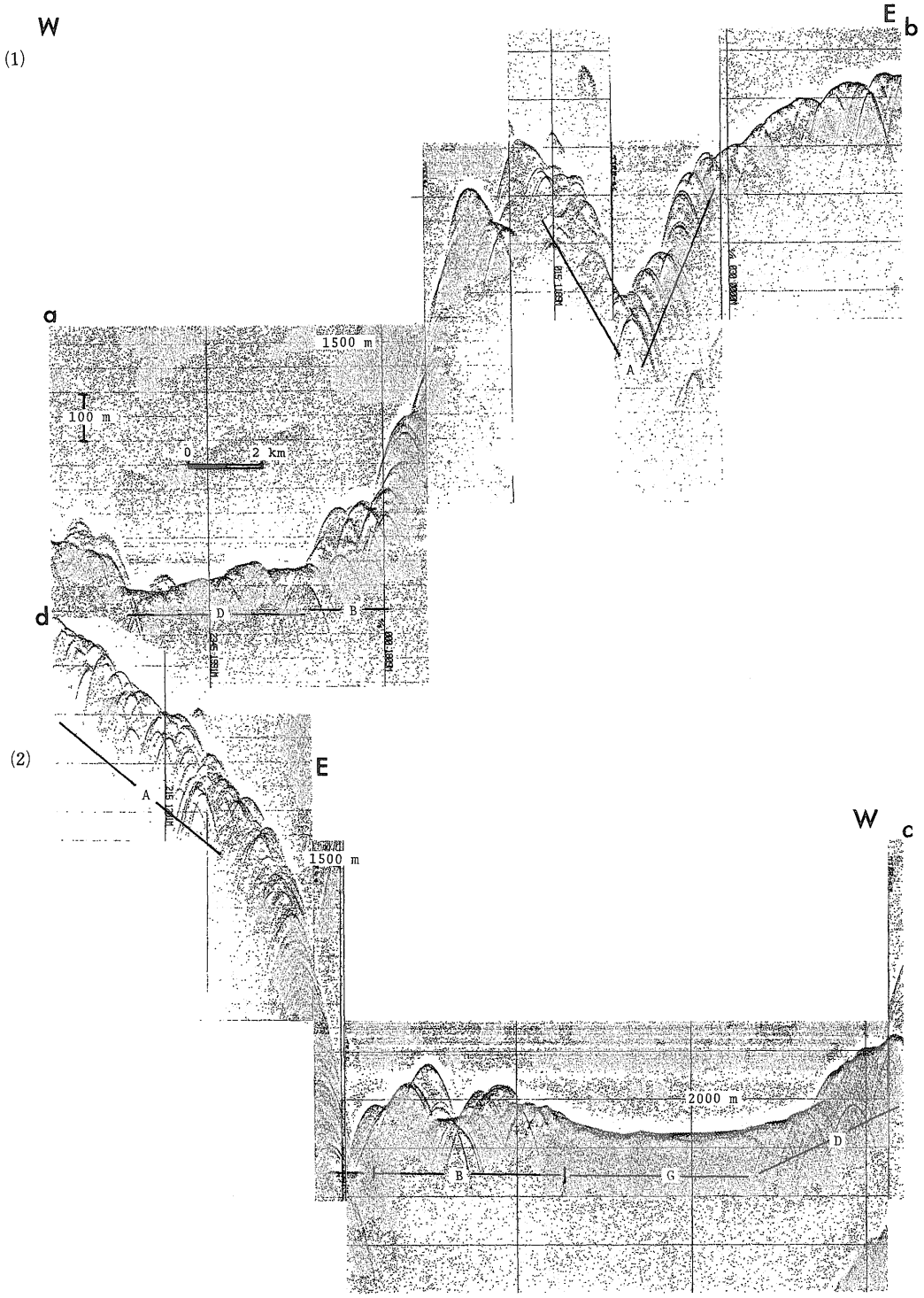

Fig. 4 (1)-(7) Typical echogram types on 3.5kHz SBP records in and around the Sumisu Rift. (A)-(H) show the echogram types. Survey lines are shown in Fig. 3

(3)

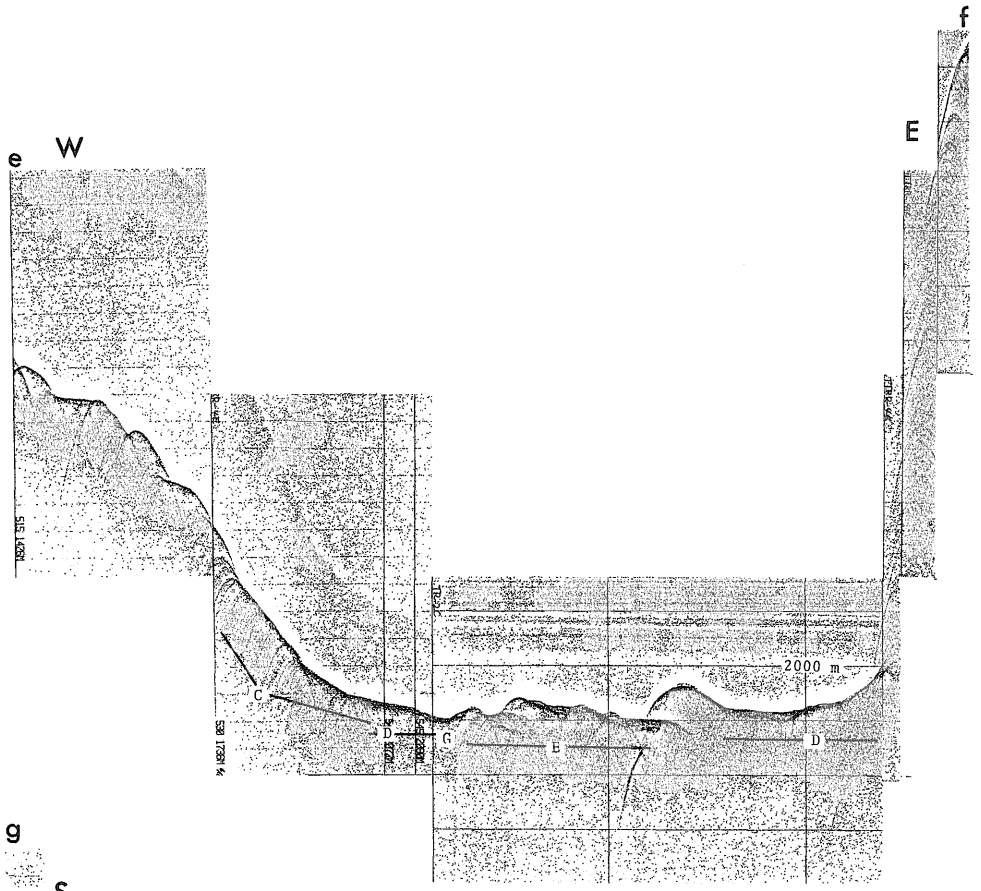

(4)

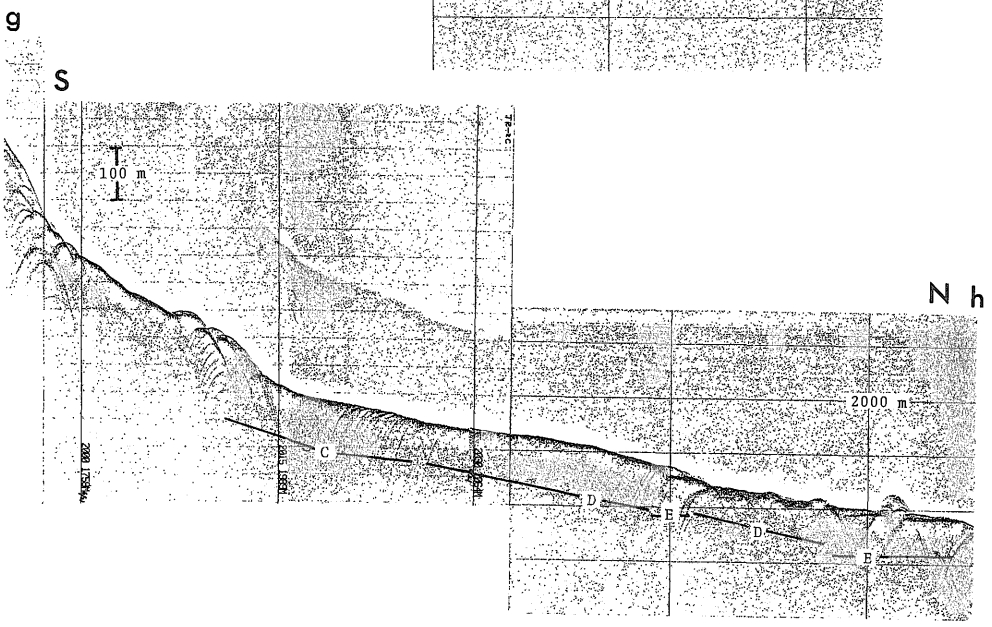

Fig. 4 continued

(5)

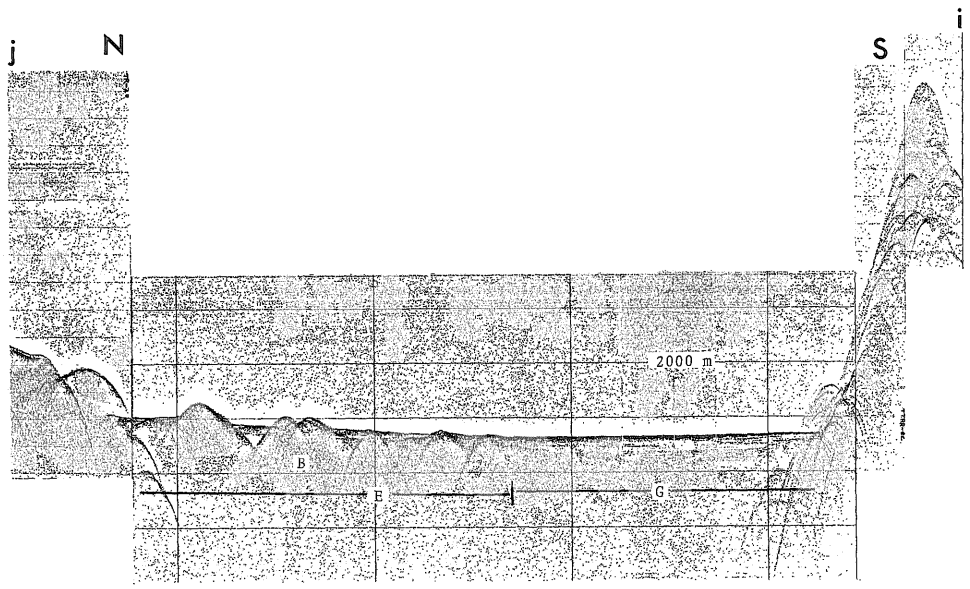

(6)

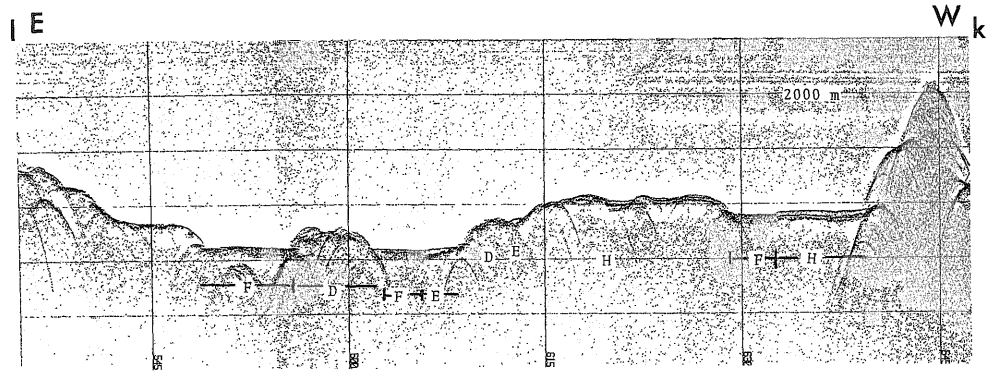

(7)

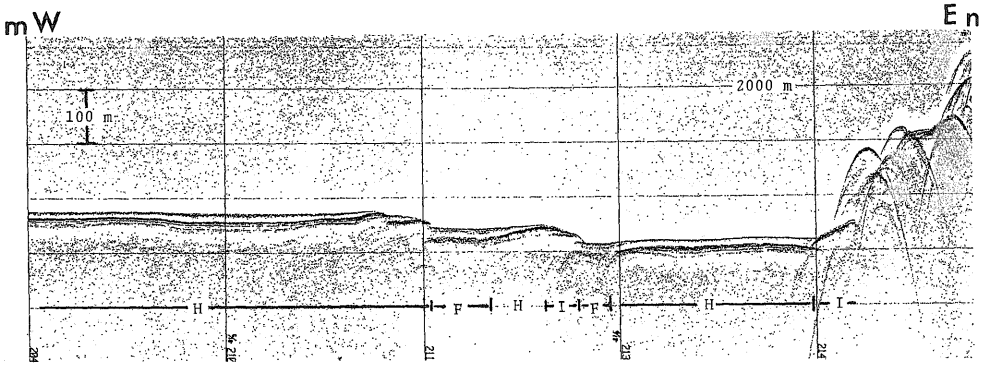

Fig. 4 continued

observations and sediment analysis, core sequences of the sediments are divided into four lithologic units (two main units and two supplementary units), as follows (Table 3). The results of grain size analysis and calcium carbonate content measurements on some samples are shown in Table 4 and Figures 5, 6, 7 and 8.

I. Hemipelagic mud

This unit occurs at the top of the core sequences in the whole area of the rift. The color is very dark grayish brown to very dark gray. Usually surface of the unit is darkest and gradually becomes lighter in the lower parts. Chemical analysis of the darker part (top of the core) show very large content of acid soluble manganese, which is greater than 0.4% at all stations and exceeds 1.0% at several stations (NAKAO *et al.*,1986). A great number of manganese micronodules and manganese oxide attached particles are observed in smear slides. The main components of this lithologic unit are terrigenous silt, clay and nannoplanktons. The component coarser than 63 μm consists mainly of radiolarian tests, volcanic glass shards, and foraminiferal tests, in decreasing order of amount. This unit shows no sedimentary structure, but shows some biogenic structures, such as, *Planolites* and *Scolicia* (Plate 1). Sediments are clayey silt on Shepard triangle (Fig. 7), and very poorly sorted (Fig. 6) fine to very fine silt with the median grain size (6.7-7.8ø). Calcium carbonate content is 8-14% and planktic foraminiferal tests in sand-sized grains are highly effected by dissolution.

I′. Hemipelagic mud with large content of calcium carbonate

This unit occurs at only one core sequence (RC452). This station is located near the distinct N-S trending faults and SBP echogram shows outcrop of sharp multiple reflectors (Type I). The color of this unit is dark gray, and components are nearly the same as those of Unit I. The dissolution effect on the calcareous forminiferal tests is not observed and calcium carbonate content (15-20%) is larger than that of unit I. As a peculiar biogenic structure, pyritized filaments are observed in the X-radiograph (Plate 1). Sediments are silty clay on Shepard triangle (Fig. 7) and very poorly sorted (Fig. 6) clay with median grain size (8.2 ø).

II. Coarser-grained volcanogenic turbidite

The color of this unit varies from pale gray to black. Grain size varies from clayey silt to coarse-grained sand. The component of this unit is mainly volcanogenic grains, such as pumices, scoriae and glass shards. The minor components of coarser grains are foraminiferal tests (both planktic and benthic), molluscan shell fragments, bryozoan fragments, radiolarians, and lithic fragments of volcanic rocks. The calcium carbonate content is less than 1.8%. The sedimentary structures observed in the X-radiographs are parallel and cross lamination, and grading (Plate 1). As a biogenic structure, a *Teichichnus* cutting lamination, is observed. Sorting is moderately well (Fig. 6).

This unit including scoria dominant layers are observed in Cores, RC321, RC330 (central part of the North Basin), and RC452 (eastern central part of the South Basin). The unit including pumice dominant layers are observed in Cores, RC325, RC397, RC322 (northern part of the North Basin) and RC343 (east-southern part of the South Basin). Core RC331 is composed of only one fragment of pumice with 8 cm long. This unit is in other cores composed of mainly glass shards.

II′. Finer-grained volcanogenic turbidite

The color of this unit is gray to dark gray. The major component of this unit is volcanogenic glass shards. The glass shards are colorless and are mostly elongated pumice type with pipe vesicles and bubble wall type. The minor component of this unit is calcareous nannoplanktons and it consistently contains less than 1.7% calcium carbonate.

Table 3 Lithologic units of the core sequences in the Sumisu Rift.

LITHOLOGIC UNIT	COLOR / TEXTURES	COMPOSITIONS		STRUCTURES IN X-RADIOGRAPH	DISTRIBUTION
		SAND GRAINS	FINE GRAINS		
		(carbonate content)			
I. HEMIPELAGIC MUD	Very dark brown -dark gray CLAYEY SILT (Md_ϕ ; 6.7-7.8)	RADIOLARIANS FORAMINIFERS (planktic & benthic) GLASS SHARDS (8-14%)	SILT-CLAY CALCAREOUS NANNO	BIOGENIC *Planolites* *Scolicia*	NORTE BASIN & SOUTH BASIN
I'. HEMIPELAGIC MUD WITH LARGE CONTENT OF CALCIUM CARBONATE	very dark gray SILTY CLAY (Md_ϕ ; 8.2)	FORAMINIFERS (planktic & benthic) RADIOLARIANS GLASS SHARDS (15-20%)	SILT-CLAY CALCAREOUS NANNO	BIOGENIC *Planolites* Pyritized filaments	CENTRAL PART OF SOUTH BASIN
II. COARSER-GRAINED VOLCANOGENIC TURBIDITE	dark gray, black, and pale gray SAND-CLAYEY SILT (Md_ϕ ; 0.9-5.2)	GLASS SHARDS PUMICE LITHICS FORAMINIFERS (planktic & benthic) SHELL FRAGMENTS (+-1.8%)	SILT-CLAY	Parallel laminated Cross laminated Graded	NORTH BASIN & CENTRAL PART AND NORTH-WESTERN MARGIN OF SOUTH BASIN
II'. FINER-GRAINED VOLCANOGENIC TURBIDITE	gray -dark gray SILT-CLAYEY SILT (Md_ϕ ; 6.7-7.0)	almost nothing GLASS SHARDS (+-1.7%)	SILT-CLAY CALCAREOUS NANNO	Thinly parallel laminated	NORTH BASIN & SOUTH BASIN

Table 4 Results of grain-size analysis and measurements of calcium carbonate content of the sediments in the Sumisu Rift.

Sample No.	depth(cm)	Size fraction(%) sand	silt	clay	Median grain size (φ)	$CaCO_3$(%)	Lithologic unit	Sysmbols in Figs.
R C321	7- 5	8.91	50.70	40.39	7.21	14.3	I	a
	55- 62	78.28	12.79	8.93	0.96	1.8	II	b
	62- 65	82.67	8.34	8.99	1.37	+	II	c
	67- 72	5.91	71.22	22.87	6.89	+	II′	d
R C324	2- 7	10.46	51.25	38.29	7.77	12.7	I	e
	51- 59	64.47	29.72	5.81	3.56	+	II	f
	90- 97	14.10	57.83	28.07	6.60	6.6	I	g
R C326	112-117	1.39	78.38	20.23	6.83	1.0	II′	h
R C396	2- 7	8.26	48.25	43.49	7.53	10.1	I	i
	67- 72	0.18	80.54	19.29	6.68	0.9	II′	j
R C334	5- 10	5.43	51.02	43.55	7.65	8.9	I	k
	90- 95	0.10	73.90	26.00	6.96	1.1	II′	l
R C335	8- 12	9.99	53.43	36.58	6.99	8.7	I	m
	87- 92	74.64	17.30	8.06	3.28	1.1	II	n
	147-152	0.33	78.24	21.43	6.89	0.8	II′	o
R C452	5- 10	8.18	53.50	38.32	7.20	10.5	I	p
	140-145	18.05	74.62	7.33	5.18	+	II	q
	150-155	9.20	37.73	53.07	8.24	15.4	I′	r
R C337	7- 12	7.87	53.63	38.50	7.25	9.0	I	s
	72- 77	1.30	77.04	21.66	6.72	1.7	II′	t
B 101	0- 2	9.62	56.07	34.31	6.70	11.5	I	u
	2- 5	9.62	56.51	33.87	6.71	12.2	I	
	5- 8	8.33	57.86	33.81	6.67	10.7	I	
	8- 12	8.20	60.52	31.28	6.60	11.0	I	
	12- 17	11.33	73.56	15.11	6.38	7.1	I	

Sediments are clayey silt and median grain size is fine silt (6.7-7.0 ø). Sorting is moderately well (Fig. 6). Thinly parallel laminations are the dominant sedimentary structure (Plate 1). Laminations are formed by darker and lighter colored parts with thickness less than 1 mm, and some laminations show undulating and cut-fill structures.

There are some transitional types of sediments between Unit I and II/Unit I and II′ with mixing of compositions and gradual change of structures, such as alternation of poorly developed laminations and biogenic structures.

5. Discussions

5.1 Sedimentation processes inferred from echogram analysis

Echogram type distribution in and around the Sumisu Rift is shown in Figure 9. Sedimentation processes which were interpreted from the echogram types in combination with their successions, associations and topographic situations, are shown in Table 2.

The North Basin; In the north-eastern, and western margins of the basin, mass flow deposits forms " mass flow wedge" with planes

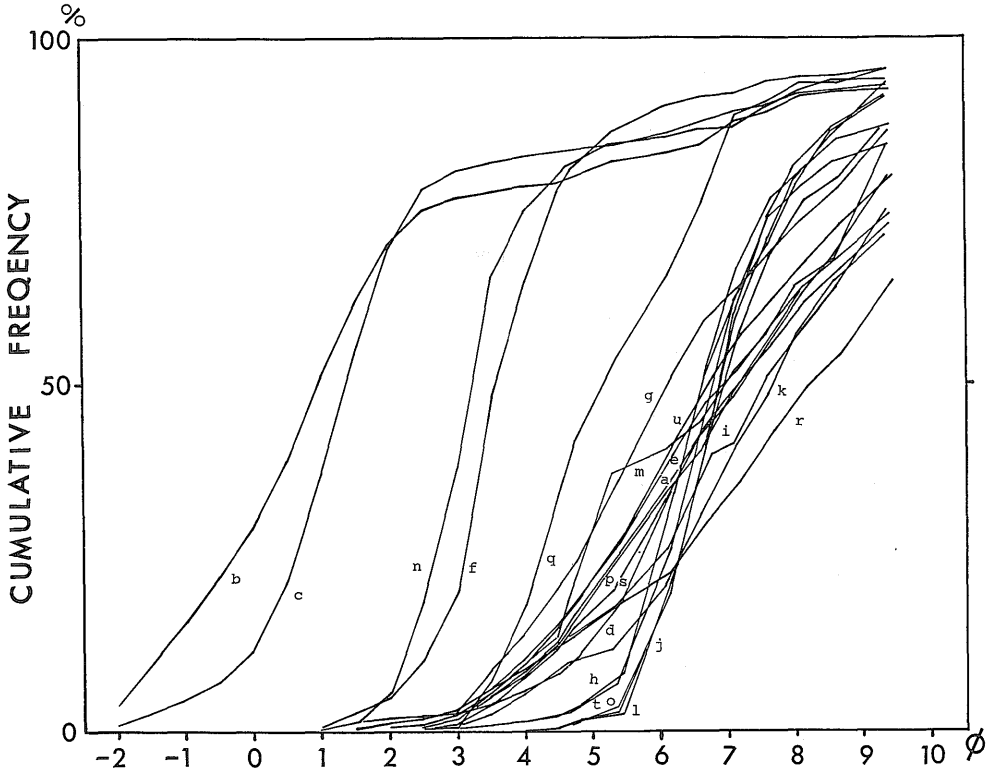

Fig. 5 Cumulative curves of grain-size distribution of sediments in the Sumisu Rift.

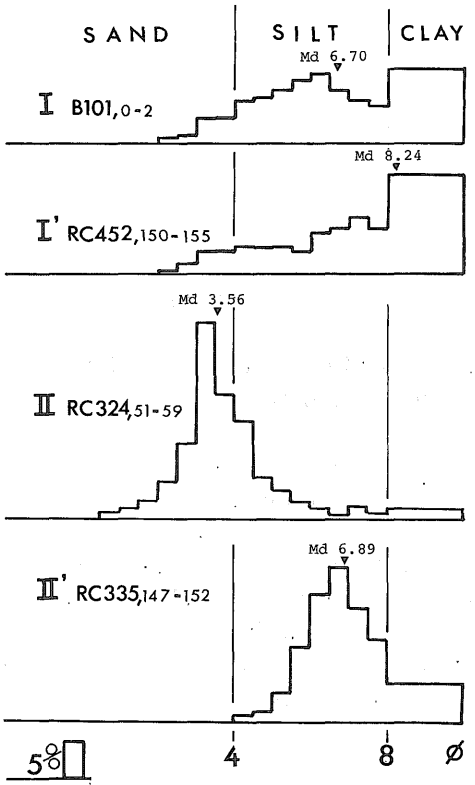

Fig. 6 Histograms of grain-size distribution of sediments of typical types of the lithologic units of the Sumisu Rift. With regard to clay size part, total amounts of clay are evenly distributed between 8 to 10 ø.

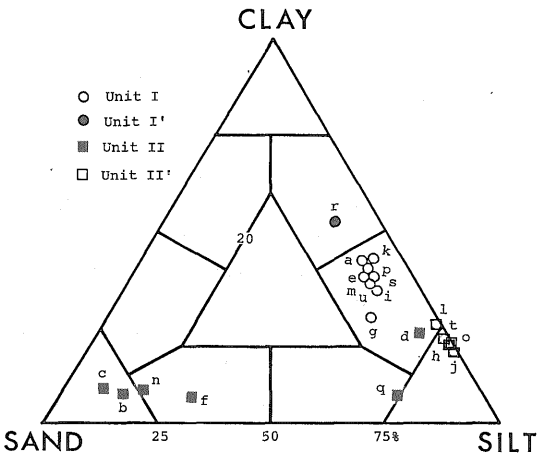

Fig. 7 Sediment types of the lithologic units of the Sumisu Rift in the Shepard triangle.

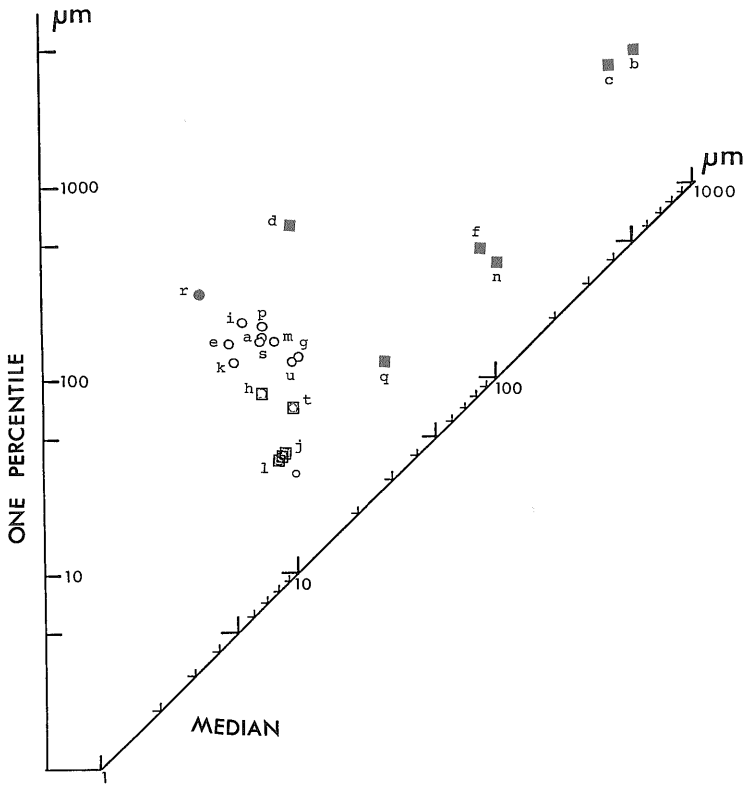

Fig. 8 Distribution of the sediments of the Sumisu Rift in the C-M diagram. Symbols are the same as that of Fig.6. Note on the distributions of Unit II and II′ almost parallel to the C = M line. Sample d (RC321, 67-72cm) shows a peculiar position on graphs (Figs. 7 and 8) which suggests the contamination of Unit II into Unit II′.

inclining towards the central part of the basin (Type C and D). In the central eastern part of the basin, "mud flow deposits" of transparent wedge (Type E) distribute and the sea floors are inclining to the south. Between the Sumisu Jima and the South Sumisu Seamount[2], a large mass wasting area supplying a vast amount of sediments to the basin is noted (BROWN and TAYLOR, 1987), but more westward slopes and valley show complicated echogram with highly crowded hyperbolae (Type A) suggesting a large block sliding. Flat basin floor is poorly developed in the western part of the basin, which is occupied by echogram type showing turbidite filling (Type G).

The South Basin; A thick and continuous blanket of transparent layer (Type H) is distributed in the whole South Basin. Many N-S trending normal faults displace the multiple layered structure under the transparent layer, and narrow depressions formed by faults are filled with transparent layer untill forming of almost flat floor. The transparent layer corresponds to hemipelagic mud and finer-grained volcanogenic layers. Transparency on seismic records is possibly indebted to the low content of calcium carbonate in the hemipelagic mud (Unit I) and finer-grains of volcanogenic sediment layers (Unit II′). On the contrary, the multiple layered structures below the transparent layer is possibly due to the fluctuation of calcium car-

2) The South Sumisu Seamount is called the Daisan-Sumisu Knoll in the bathymetric chert "Sumisu Sima".

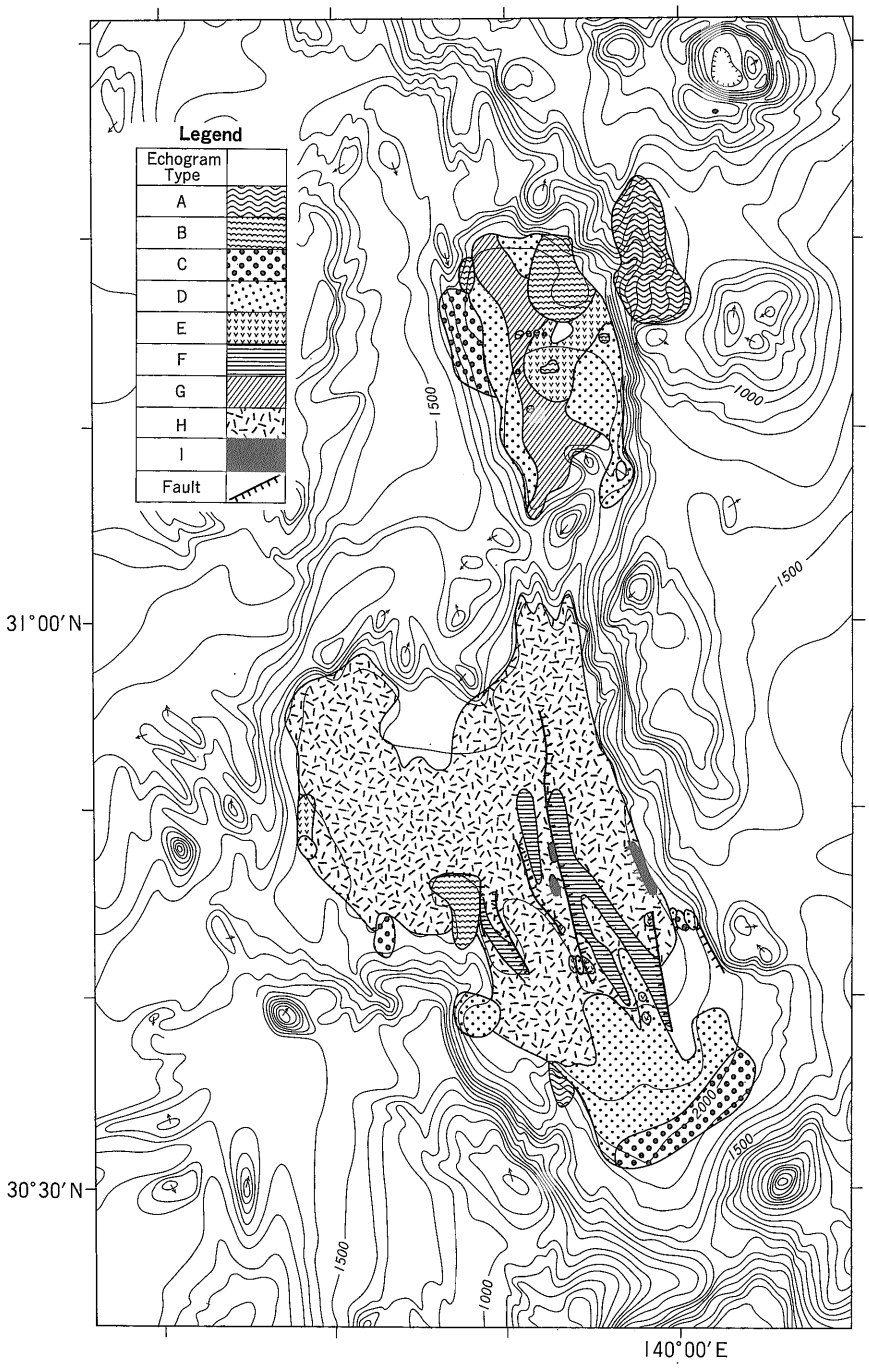

Fig. 9 Distribution of the echogram types in the Sumisu Rift.

bonate content in hemipelagic mud producing acoustic impeadance variety of sediments (MAYER, 1979). It is pointed out that periodic influxes of pyroclastic and/or epiclastic sediments or changes in bottom currents may contribute the layered structures (BROWN and TAYLOR, 1988) but the uniformity of the echogram suggests that they have been formed through the pelagic sedimentation processes. Between the southern margin of the basin and the line of mountains west of the Torishima Island, echogram types related to sliding and debris flow sedimentation distribute. In southern to central eastern part of the basin, narrow depressions forming by fault displacement are burried by turbidity current deposits (Type F). Core, RC343, which was taken from the area with Type F echogram, has coarse thick volcanogenic sediments (Unit II) in the lower part of the sequence.

5.2 Sedimentation processes inferred from core sediments

The names of lithological units used in the previous section already imply genetic meanings. The Unit I and I′ have hemipelagic nature which is inferred from their compositions, dominant terrigenous finer-grained particles and biogenic particles, and grain texture, poorly sorted clayey silt to silty clay. The sediments of Unit I and I′ deposited through the ordinal process from the suspended terrigenous and biogenic material. The difference of calcium carbonate contents between the Unit I and I′, suggests the change of the bottom environment between the depositional periods of the units. This change is possibly referred to the increase of corrosive nature in bottom water in the Pacific Ocean after the last glaciar (BERGER, 1973). As another possibility of the cause, local environmental changes, such as increasing of organic productivity and oxigene content of bottom water, need attensions, because of fairly shallower depth of the basins. In the Japan Sea, CCD fluctuation and foraminifer poor sediments have been related to injected water with high oxigene content and high organic productivity in the latest Pleistocene through to the Recent (KITAZATO, 1984). Peculiar biogenic structure, pyritized filaments, and thin shell species dominant benthic foraminiferal assemblage in Unit I′, suggest relatively reduced condition and the darker color of surface sediments (Unit I) shows highly oxidized condition. The change from reduced to oxidized condition possibly occurred between the depositional periods of the two units in bottom water of the basin. This change has inferred the change of the content of calcium carbonate in sediments.

The Unit II and II′ are almost composed of volcanogenic particles. The sedimentation processes of these units is concluded to be turbidity current by following reasons. (1) The sedimentary structures observed in these units, such as graded, cross laminated, parallel laminated structures are common in turbidite sequences (BOUMA, 1962). (2) Components derived from shallower part, such as benthic foraminifers and shell fragments, are found in these units. The calcareous nannoplanktons included in the unit II′ has the origin of slope/shallower sediment as the same shallower components of the Unit II and separated from the coarser components by the uniform grading processes of turbidity current system which is shown in the parallel distribution of Unit II and II′ to C=M line in C-M diagrams (Fig. 8).

It is very difficult to recognize the sequence formed by one turbidity flow in Unit II′, because of the lack of a distinctive succession of sedimentary structures except thin parallel laminations. The color contrasts at one to several centimeters thick possibly correspond to the sediments formed by respective turbidity flows. The lack of hemipelagic mud in subsequent volcanogenic turbidites of Unit II and II′ implies that the turbidity currents had subsequently occurred in and just after the eruptions which supplied a vast amount of

the volcaniclasts.

The origin of volcaniclastic particles are thought to be mainly arc volcanoes. Vast amount of pyroclastic sediments in the basin suggested their origin from near the intra-rift volcanoes (FUJIOKA, 1983). The highly vesiculated volcanic rocks with value of 60% in maximum were taken from the intra-rift volcanoes (FRYER *et al.*,1986). Volcanogenic components in sediments in the core sequences are composed of mainly glass shards derived possibly from subaerial eruptions and/or subaqueous ones above PCL (pressure compensation level). And no evidence of contribution of intra-rift volcanoes to the basin sediments was found. The volcaniclastic components have been probably supplied from the volcanoes on and around the Sumisu Jima and the Tori Shima Island of volcanic chain. With regard to land samples of the Sumisu Jima and the Tori Shima Islands, mafic volcanic rocks are dominant (KUNO, 1962 ; ZHANG *et al.*,1986) but dacite lava and pumices were taken from dredged hauls around the islands (Geological Survey of Japan, 1985).

The distribution of the lithologic units in the basins is shown in Fig.10. Coarser volcanogenic sediments (Unit II) are dominant in the North Basin and are restricted in the eastern and southern margins of the South Basin. Finer volcanogenic sediments (Unit II′) are distributed in the whole basins, and the Unit II′ in the South Basin shows poor development of thin laminations except in the western margin of the basin.

5.3 Comparison of sedimentation between the two basins

The distributions of echogram types and lithologic units reveal the differences of the sedimentary environments of the basins. In the North Basin, echograms show the dominance of gravity flow sedimentation processes in burying the basin, and the sediments of the basin are much coarser than those in the South Basin. In the South Basin, echograms show the hemipelagic deposition and sediments of the basin rather finer than those in the North Basin except in the southern and the western margins.

Environments inferred from the analysis of echogram and lithology in the two basins are different. The North Basin shows "oversupplied basin plains" and the South Basin "under supplied basin plains"(STOW, 1985). Because the tectonic settings of the two basins are thought to be almost same, this difference is indebted to the topographical differences in and around basins deciding the supply of the sediments from the arc volcanoes. The North Basin is a narrow basin with N-S axis parallel to the volcanic arc trend and about half the size of the South Basin and is directly buried through a gravity flow sedimentation caused by a vast supply from the arc volcanoes, such as the Sumisu Jima and its surrounding mountains. With regard to the South Basin, the broad slope along the southern margin of the basin to the line of the ridge west of the Tori Shima Island has possibly entrapped the vast supply of the volcaniclastics from the arc volcanoes. And, echograms on E-W survey lines across the slope show alternating topography of troughs and bars suggesting a possibility of fan formed by turbidity currents.

6. Conclusions

The analysis of the sediments and the echogram on 3.5-kHz SBP reveal the following natures of sedimentation in the Sumisu Rift.

1. Echogram type distribution of the North Basin implies that sliding, debris flow, and turbidity flow have contributed in the sedimentation.
2. On the contrary, echogram type distribution of the South Basin, shows rather quiet condition, such as hemipelagic sedimentation accompanied with some turbidity current and gravity flow ones.
3. Core lithology of the basins is the

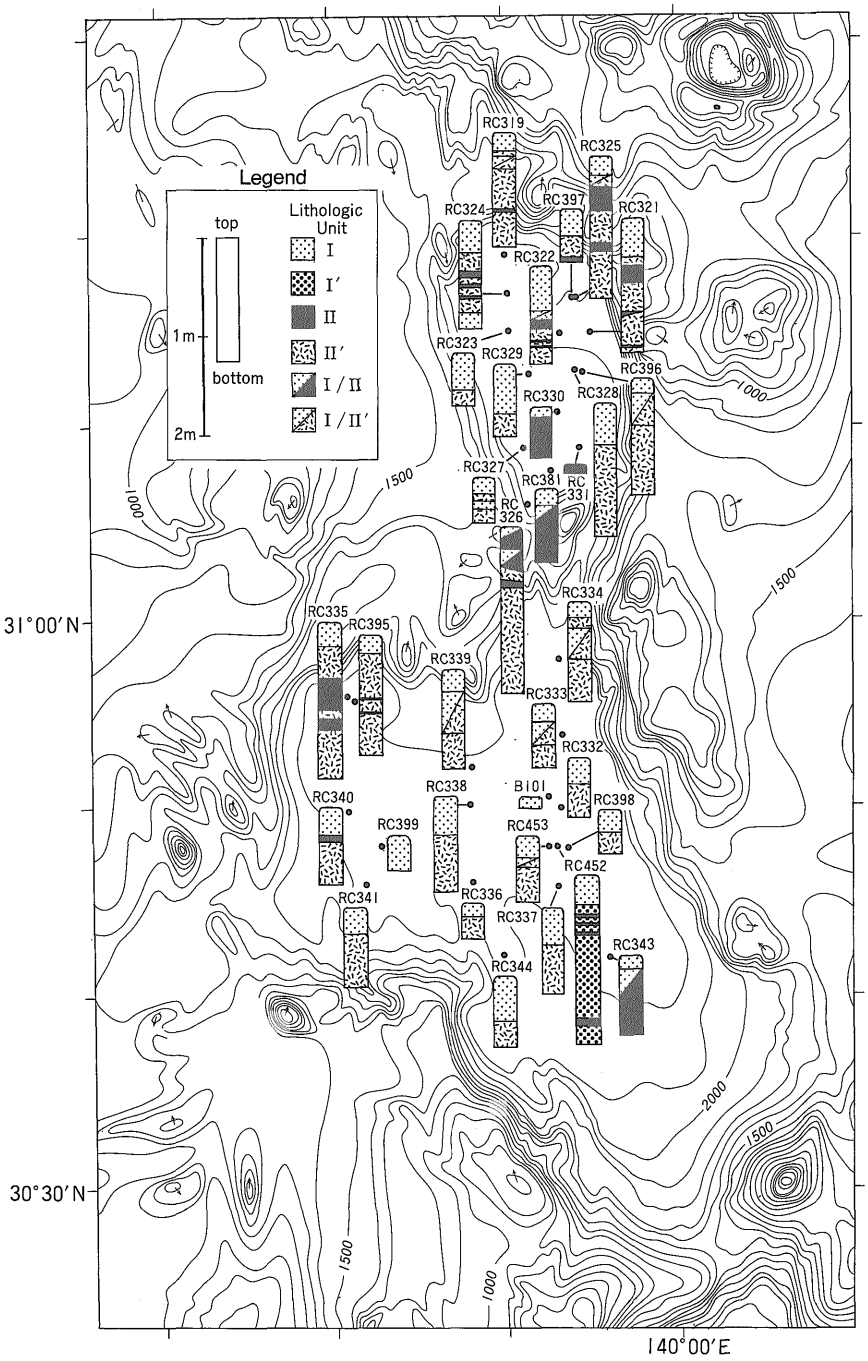

Fig. 10 Distribution of the lithologic units in the Sumisu Rift.

hemipelagic mud and volcanogenic turbidites in both the basins. Coarser volcanogenic turbidites are more common in the North Basin corresponding to the difference of gravity flow contribution implied by echogram types.

4. The sampled surface sediments in the both basins are composed of hemipelagic mud showing present quiet condition. And the volcanogenic turbidites dominated in the lower core sequences implies the active periods of volcanic eruptions, which had supplied vast amount of the volcaniclastics to the slopes around the basins.

5. The differences of sedimentation processes and natures between the basins, which are situated on the nearly equal tectonic setting, are indebted to the topography of the basin and surrounding slopes, and the amount of supply of the sediments mainly from the eruptions of the arc volcanoes.

To draw the actual sedimentation process of the rift, dating and exact correlation of the volcanogenic sediment components with the pyroclastics and lavas of subaerial and submarine arc volcanoes, are needed.

Acknowledgements : This work was carried out through the special research program funded by the Agency of Industrial Science and Technology, MITI, "Submarine Hydrothermal Activity in Izu-Ogasawara Arc" , which has been conducted by S. N AKAO and M. YUASA. B. TAYLOR and G. BROWN of the University of Hawaii kindly offered their manuscript of the work on the Sumisu Rift. M. NOHARA encouraged the authors and reviewed the manuscript. M. TANAHASHI, G. BROWN, Y. SHIMAZAKI, S. NAKAO, and Y. SAITO reviewed the manuscript. We thank the researchers mentioned above and all staffs of the project and crew members of R/V Hakurei-Maru.

References

BERGER, W. H. (1973) Deep-sea carbonates: Pleistocene dissolution cycles. *J. Foram. Res.*, vol.3,p.187-195.

BOUMA, A. H. (1962) Sedimentology of some flysch deposits. Elsevier, Amsterdam. 168pp.

BROWN, G. and TAYLOR, B. (1988) Sea-floor mapping of the Sumisu Rift, Izu–Ogasawara (Bonin) Island Arc. *Bull. Geol. Surv. Japan*, vol.39,p.23-38.

CAREY, S. and SIGURDSSON , H. (1984) A model of volcanogenic sedimentation.: KOKELAAR, K. P. and HOWELLS, M. F.(eds.) Marginal basin geology. Geol. Soc. London, Spec. Publ., no. 16, p.37-58.

DAMUTH, J. E. (1980) Use of high-frequency (3.5-12kHz) echograms in the study of near-bottom sedimentation processes in the deep-sea : a review. *Mar. Geol.*, vol. 38, p.51-75.

FRYER, P., LANGMUIR, C., TAYLOR, B., ZHANG, Y., and HUSSONG, D.(1986) Rifting of the Izu Arc , Ⅲ : Relationship of chemistry to tectonics. *Trans. Am. Geophys. Un.*,vol.66,p.421.

FUJIOKA, K.(1983) Where were the "Kuroko deposits" formed, looking for the present day analogy. *Mining Geol., Spec. Issue*, no.11,p.55-68. (in Japanese with English abstract)

Geological Survey of Japan (1985) Research on "Submarine Hydrothermal Activity in Izu-Ogasawara Arc"–1984 FY Report–. 99p. (in Japanese)

HONZA, E. and TAMAKI, K. (1985) Bonin Arc.; NAIRN, A. E. M., STEHLI, F. G. and UYEDA, S. (eds.) The ocean basins and margins, vol.7A, The Pacific Ocean, p.459-502.

JACOBI, R. D. (1976) Sediment slides on the Northwestern continental margin of Africa. *Mar. Geol.*, vol. 22, p.157-173.

KITAZATO, Y. (1984) Fluctuation of CCD. – on the analysis of core sample, C-3, KH79-3. *Chikyu, monthly*, vol.6, p.567-570.(in Japanese)

KUNO, H. (ed.) (1962) Catalogue of active volcanoes of the world including solfatara fields, part 11. 332p.

MAYER, L. A. (1979) Deep sea carbonates: acoustic, physical, and stratigraphic properties. *Jour. Sed. Petr.*, vol.49,p.819-836.

MURAKAMI, F. (1988) Structural framework of the Sumisu Rift, Izu-Ogasawara Arc. *Bull. Geol. Suev. Japan*, vol .39,p. 1 -21.

NAKAO, S., MITA, N., NISHIMURA, A. and YAMAZAKI,T. (1986) Chemical compositions of surface sediments and heat flow data of the back-arc depressions of the Izu-Ogasawara Arc. Abst. 93rd. Annual Meeting, Geol. Soc. Japan, 93, p.276.(in Japanese)

——— and YUASA, M. (ed.) (1986) Research on "Submarine Hydrothermal Activity in Izu-Ogasawara Arc" –1985 FY Report–. 149p. Geological Survey of Japan. (in Japanese)

——— and YUASA, M. (ed.) (1987) Research on "Submarine Hydrothermal Activity in Izu-Ogasawara Arc"– 1986 FY Report–.184p. Geological Survey of Japan. (in Japanese)

SIGURDSSON, H. and CAREY, S. N. (1981) Marine tephrochronology and quaternary explosive volcanism in the Lesser Antilles Arc.: SELF, S and SPARKS, R. S. J. (eds.) Tephra Studies, p.255-280.

STOW, D. A. V. (1985) Deep-Sea clastics: where are we and where are we going? : BRENCHLEY, P. J. and WILLIAMS, B. P. J. (eds.) Sedimentology: Recent developments and applied aspects. Geol. Soc. London, Spec. Publ., no.18, p.67-93.

TAMAKI, K., INOUE, E., YUASA, M., TANAHASHI, M. and HONZA, E. (1981) Possibility of the back-arc spreading in the Ogasawara Arc, during the Quaternary Period. *Chikyu, monthly*, vol.3, p.421-431.(in Japanese)

ZHANG, Y., LANGMUIR, C., TAYLOR, B., FRYER, P. and HUSSONG, D. (1986) Active volcanism in the Izu Arc and Rift, II: The volcanic front. *Trans. Am. Geophys. Un.*, vol.66, p.421.

伊豆・小笠原弧，スミスリフトにおける堆積作用

西村　昭・村上文敏

要　旨

伊豆・小笠原背弧のスミスリフトにおいて，柱状採泥試料と 3.5kHz サブボトムプロファイラー（ＳＢＰ）記録により堆積作用を検討した．同リフトの北海盆では，ＳＢＰ記録は重力流による埋積を示唆し，海盆底は小起伏や傾斜した平坦面からなる．同じく南海盆では，ＳＢＰ記録は南東部での重力流堆積作用の存在と平坦な海盆底での透明層と稿状構造が遠洋性懸濁からの堆積を示唆する．海底表層の柱状試料の岩相は，両海盆とも，上部の半遠洋性泥と下部の火山性砕削物のタービダイトからなり，北海盆の方が粗粒の火山源粒子が多い．これらは，現在の静穏な時期と過去の大量の火砕物質が供給され重力流堆積作用のあった火山活動の活発期を示す．両海盆の堆積物の差異は，堆積物の供給に関連した地形的な要因が大きいと推察される．

（受付：1987年４月９日；受理：1987年11月６日）

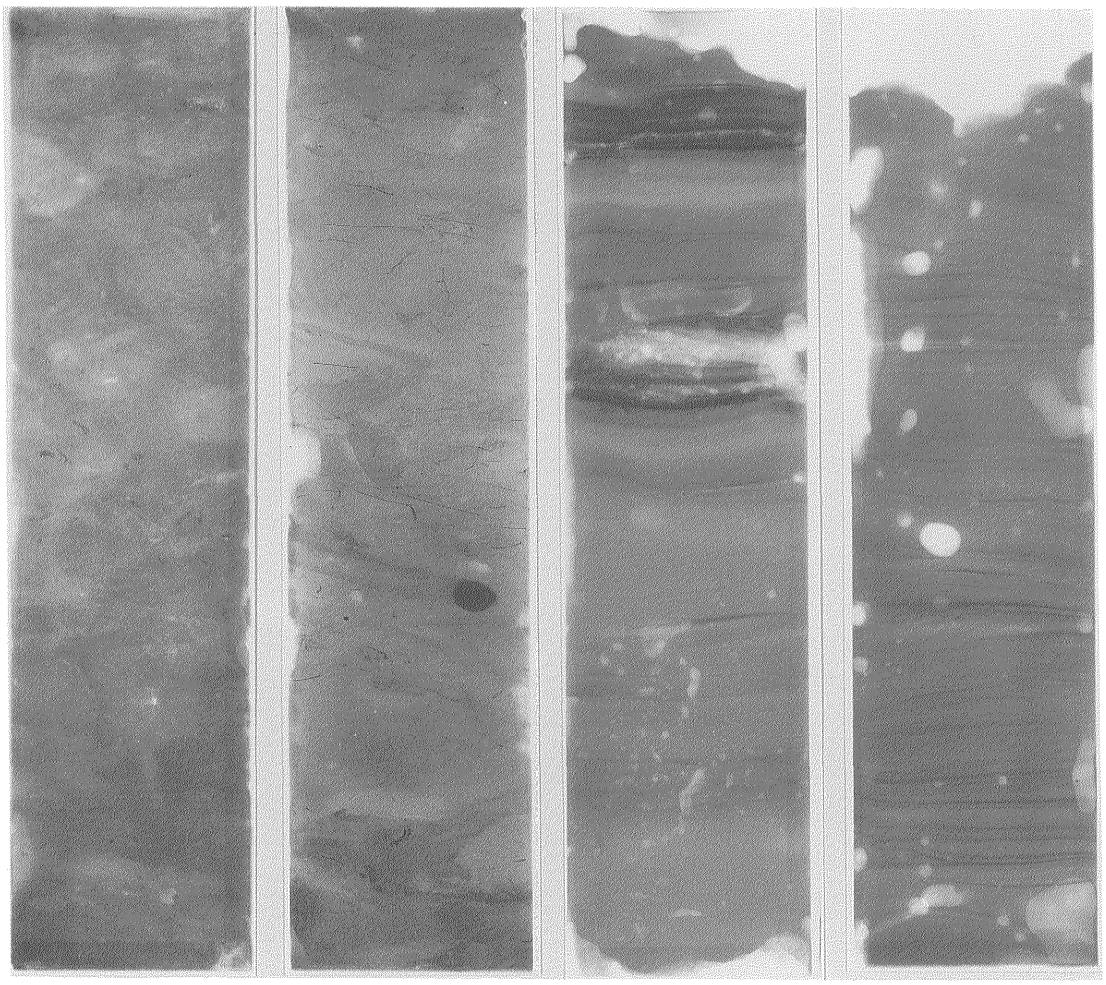

Plate 1 X-radiographs of the lithologic units in the Sumisu Rift.

1. Unit I, RC321, 12-32 cm.
2. Unit I′, RC452, 133-153 cm.
3. Unit II, RC322, 53-73 cm.
4. Unit II′, RC326, 122-142 cm.

Heights and widths of figures are 20 cm and 5 cm, respectively.
Bubble-like shapes on figs. 3 and 4 (white circles) are artificial structures through the preparation of the sediment slices.